IET Electric Power Applications, 2010, Volume 4, Issue 8, pp647-656

Cogging torque suppression in a permanent-magnet flux-switching integrated-starter-generator

M.J. Jin[1] Y. Wang[1] J.X. Shen[1] P.C.K. Luk[2] W.Z. Fei[2] C.F. Wang[1,2]

[1]College of Electrical Engineering, Zhejiang University, Hangzhou 310027, People's Republic of China
[2]Department of Engineering Systems and Management, Cranfield University, Shrivenham SN6 8LA, UK
E-mail: j_x_shen@zju.edu.cn

Abstract: Permanent-magnet flux-switching (PMFS) machine offers high torque density, impressive flux-weakening capability and mechanical ruggedness because of its distinctive configuration, and is potentially suitable for the application in automotive integrated-starter-generators (ISGs). However, the PMFS machine generally exhibits higher cogging torque compared with other machines commonly used in ISGs. Minimisation of the cogging torque in the PMFS machine for its utility in ISGs is therefore of particular importance. Four rotor topologies are proposed here as cost-effective means to suppress the cogging torque of a PMFS ISG. The validity of the proposed techniques has been confirmed by both two-dimensional finite-element analysis and experimental results. Moreover, the influence on the back electromagnetic force by these techniques is also investigated.

1 Introduction

Integrated-starter-generators (ISGs) are normally a highly power dense and efficient electric drive with multi-quadrant operational capability, which can be employed to replace the conventional separated starter and generator in modern road vehicles [1]. Various electric machine types have been surveyed and proposed for ISG applications [2]. In general, the ISG should be capable of offering a very high starting torque for cold cranking and a constant output voltage over a very wide speed range for battery charging. The permanent magnet (PM) brushless machine has been considered as the most competitive candidate for ISG applications because of its high power density and efficiency. However, owing to the extreme temperature under the hood of the vehicle, the PM machine is particularly vulnerable to poor temperature management, which may result in degradation in machine performance, and even severe demagnetisation of the magnets in machine's rotor in the extreme cases.

The permanent-magnet flux-switching (PMFS) machine is a doubly salient machine comprising a passive rotor and a stator with both windings and PMs. The variety of methods to accommodate the windings and PMs within the stator offers many design options for the PMFS machines [3, 4]. Because of its unique structure, the PMFS machine inherits such merits as high torque density, good efficiency and excellent flux-weakening capability from the conventional interior PM brushless machine, and the ruggedness of the rotor from the switched reluctance machine. Furthermore, effective thermal management can be readily achieved since the crucial parts of the machine such as windings and magnets are located in the stator rather than in the rotor. Recently, a general purpose three-phase PMFS machine has been proposed to highlight its potential in ISG applications [5]. However, cogging torque in the PMFS machine is relatively high compared with other types of PM machines as a result of the high air-gap flux density produced by the magnets and the doubly salient structure, which might conduce to mechanical

vibration and acoustic noise. Thus, minimisation of cogging torque is of particular importance for the PMFS to be considered as a viable candidate for IGS applications.

To date, research on the PMFS machine has been mainly focused on general electromagnetic design procedure and performance analysis [4–19], with relatively exiguous effort addressing the issues on cogging torque reduction [20, 21]. On the other hand, for conventional PM-rotor machines, numerous techniques such as stepped rotor skewing, stator tooth width and rotor magnet spacing, teeth notching, magnets pairing and magnets shifting have been proposed to alleviate the cogging torque effects [22–24]. As a low-noise smooth start function is highly desirable in the ISG application, it is important that the PMFS provides a smooth torque quality with minimal cogging torque.

In this paper, four rotor-based cogging torque reduction techniques, namely rotor tooth-notching, rotor tooth-chamfering, rotor tooth-pairing and rotor tooth-skewing, are investigated for their utility in PMFS ISG applications. Since the PMFS machine has a complex stator structure and a simple passive rotor, it is proposed to implement cogging torque reduction by varying the rotor structure against a constant stator structure. By developing two-dimensional (2-D) finite-element analysis (FEA) models for the machine with varying rotor structures, the cogging torque and back electromagnetic force (EMF) performance of each of the techniques are evaluated and optimised. The results from the FEA models are compared with the experimental results. A good agreement between the results confirms the validity of the 2-D models. The results from the prototypes also demonstrate that the proposed techniques can be implemented very cost effectively in suppressing the cogging torque of the PMFS ISG.

2 Basics of PMFS ISG

The PMFS machine under study is based on an earlier investigation in which detailed design and analysis have been undertaken [5]. This is a further investigation into the applications and experimental verifications of the proposed cogging torque reduction techniques to the machine. The stator and rotor of the PMFS machine is depicted in Fig. 1, which shows a 10-pole rotor and a 12-pole stator comprising laminations, magnets and concentrated winding coils. The rotor is reminiscent of that of the switched reluctance motor (SRM). The main design parameters of the machine are given in Table 1. The design parameters of the stator and rotor poles are denoted in Fig. 2. In the original model of an inner-rotor PMFS machine [4], the stator pole is evenly divided into three parts, namely the lamination slot, the magnet and the lamination tooth, which also have the same width as the rotor pole. The

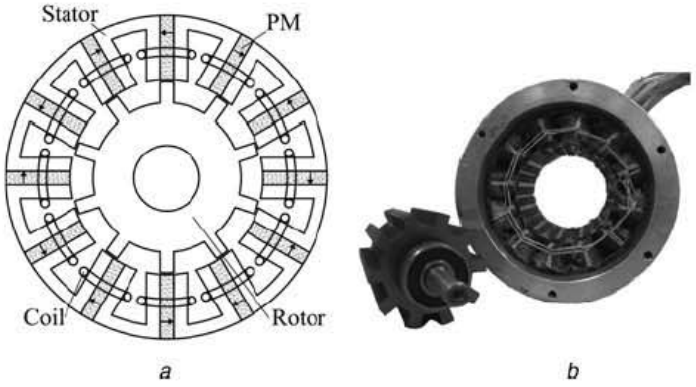

Figure 1 *Topology and prototype of proposed PMFS ISG*

a Topology
b Prototype of stator and original rotor

Table 1 Main design parameters of the proposed PMFS ISG

Symbol	Machine parameter	Value	Unit
N_s	stator pole number	12	
N_r	rotor pole number	10	
R_{so}	stator outer radius	46.00	mm
R_{si}	stator inner radius	25.25	mm
R_{ro}	rotor outer radius	24.75	mm
g	air-gap length	0.50	mm
h_{pm}	magnet width	3.24	mm
h_{pr}	rotor tooth height	6.06	mm
β_r	rotor tooth width	5.18	mm
l_a	machine active length	60.00	mm
	permanent magnet material	NdFeB35	

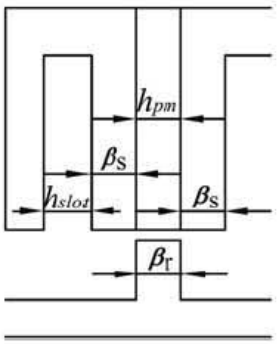

Figure 2 *Illustration of stator and rotor poles*

correlations of the parameters can thus be derived as

$$\begin{cases} h_{\text{slot}} = \beta_s = \beta_r = h_{\text{pm}} \\ \theta_s = 2\beta_s + h_{\text{pm}} \end{cases} \quad (1)$$

where β_r, h_{slot}, β_s and h_{pm} are the dimensions for the rotor tooth, stator slot, stator tooth and the magnet, respectively, while θ_s is the stator pole width. However, such relationships may not be the optimal configuration in practice [7, 8].

Thus, for the PMFS machine under study, it was proposed to have $\beta_r = 1.6\beta_s$ to improve the machine performance [5].

In the PMFS machine, the torque acting on each stator pole with open-circuit windings can be expressed as

$$T_{\text{single}}(\theta) = \sum_{n=1}^{\infty} T_n \sin(nN_r\theta) \tag{2}$$

where T_n is the amplitude of the torque of the corresponding nth harmonic and θ is the rotor position. Thus, the resultant cogging torque of the machine can be calculated by simply synthesising the torque acting on each stator pole as

$$T(\theta) = \sum_{n=1}^{\infty}\left\{ T_n \sin(nN_r\theta) \sum_{k=0}^{N_s-1} [\cos(2\pi k n N_r/N_s)] \right\} \tag{3}$$

By inspection, it is noted that the terms on the right side of (3) are all equal to zero except those in which nN_r/N_s are integers. In other words, only the terms where nN_r are the multiples of the lowest common multiple of N_r and N_s, lcm(N_r, N_s), exist. Hence, the mechanical angle corresponding to each period of the cogging torque can be obtained as

$$\alpha_{\text{cogging}} = \frac{2\pi}{\text{lcm}(N_r, N_s)} \tag{4}$$

The α_{cogging} for the machine under study can be easily derived as $\pi/30$.

To verify the results above, the cogging torque of the PMFS is evaluated by both FEA model and by measurement. The FEA-predicted and experimental results are shown in Fig. 3, in which good correlations are observed. The discrepancy between the two results is likely due to the considerable 3-D end-effects for a machine with a relatively short axial length compared with its diameter, which have not been modelled in the 2-D FEA model. Also, there are manufacture and assembly deficiencies in the prototype machine. It can be noted that the experimental peak-to-peak cogging torque is rather high, reaching almost 1 Nm. This should be addressed during

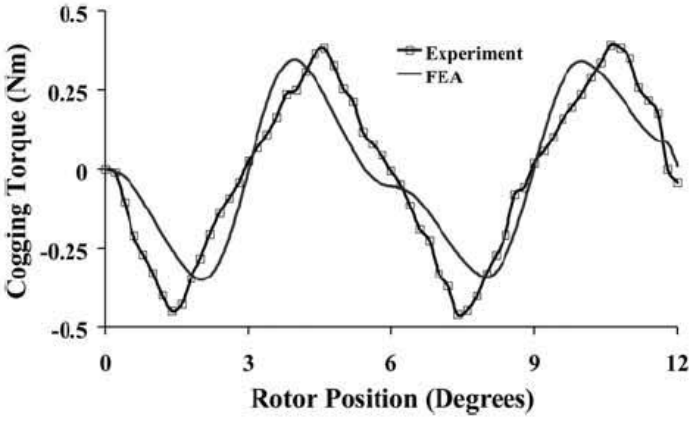

Figure 3 *Cogging torque profiles of the proposed PMFS ISG*

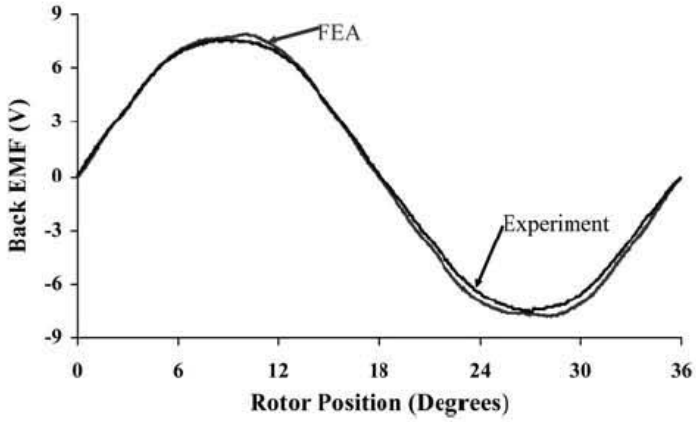

Figure 4 *Phase back EMF waveforms of the proposed PMFS ISG*

the machine design stage for an IGS application. The predicted and measured values of the phase back EMF waveforms at 1000 rpm are illustrated in Fig. 4, which shows the predicted value is slightly higher than the measured, which may also be due to neglect of the end-effects. Essentially, the results show that the back EMF is close to sinusoidal with negligible harmonic distortion, indicating that the proposed PMFS ISG is inherently suitable for brushless AC operation, that is, sine-wave operation.

3 Rotor designs for cogging torque reduction

In general, the choice of a cogging torque reduction technique depends on whether it meets the requirements of easy implementation with minimum extra costs and compromise of other machine performance. Since it is more costly and difficult to apply design techniques on the complex stator of the proposed PMFS, it is proposed to vary the rotor structures in order to implement the various cogging torque reduction schemes. From (3), it can be inspected that the overall cogging torque could be drastically reduced by minimising selected T_n through ingenious rotor structure design. Furthermore, the cogging torque can be calculated, with the energy method, as the mean value of the Maxwell stress tensor on the whole air-gap volume [25], that is

$$T(\theta) = -\frac{\partial W(\theta)}{\partial \theta} = -\frac{\partial}{\partial \theta}\left\{ \frac{1}{4\mu_0}(R_{si}^2 - R_{ro}^2) \int_0^{L_{ef}} \int_0^{2\pi} G^2(\alpha, z) B^2(\alpha, \theta) \, d\alpha \, dz \right\} \tag{5}$$

where μ_0 is the air permeability of air, α is the angle along the air-gap circumference, L_{ef} is the effective axial length of the machine, z is axial position along the machine axis; $G(\alpha, z)$ and $B(\alpha, \theta)$ are air-gap relative permeance and the air-gap flux density in an equivalent slotless machine, respectively. The magnets are located in the stator of PMFS ISG, while

in this paper the stator is not changed but the rotor is modified. Therefore $B(\alpha, \theta)$ is unchanged, but $G(\alpha, z)$ is varied with different rotor designs in order to reduce the cogging torque. In this section, four common cogging torque reduction techniques that have been applied successfully in other PM machines will be used in the design of the passive rotors for the PMFS ISG application.

3.1 Rotor tooth-notching

Cogging torque can be effectively reduced by introducing notches to create dummy slots in either the stator of surface-mounted PM machine [22] or in the rotor of interior PM machine [26]. Tooth-notching can also be applied to the PMFS machine rotor, which will increase the variation periods and decrease the variation amplitude of $G(\alpha, z)$ in (5), resulting in a reduced peak value of the cogging torque. However, this may also compromise the back EMF of the machine as a result of the enlarged equivalent air-gap length. Thus, both the number and geometric configuration of the notches should be carefully selected to minimise the cogging torque and at the same time to keep the back EMF as high as possible.

In this paper, two and three notches on each rotor tooth are selected, respectively, to reduce the cogging torque of the proposed PMFS ISG, as shown in Fig. 5. Furthermore, the notch depth h is chosen as half of the notch width l to simplify the modelling process and calculation. Consequently, the machine with two notches allocated at the positions 1/6 and 5/6 of the rotor-tooth width and with the width $l = 1$ mm is denoted as 'notch1', whereas the one with three notches allocated at the positions 1/6, 1/2 and 5/6 of the rotor-tooth width and with $l = 1$ mm is denoted as 'notch2'. Furthermore, the machine which is similar to 'notch2' but with $l = 0.8$ mm is denoted as 'notch3'. The cogging torque and phase back EMF waveforms of these machines are shown in Figs. 6 and 7, respectively. It can be seen that the three-notch structure can reduce the cogging torque much more effectively than the two-notch. However, the three-notch structure normally results in a lower back EMF. It can also be seen from Fig. 6 that both the amplitude and phase angle of the cogging torque profiles vary along with the notch width. Moreover, the polarity of the cogging torque changes when the notch width changes from 'notch2' to 'notch3'. Therefore an optimal notch width can be found between 'notch2' and 'notch3' as being $l = 0.9$ mm, which is denoted as 'notch4'. From Fig. 6, it can be seen that 'notch4' can reduce the peak of cogging torque to just 10% of the original one. However, from Fig. 7, it also degrades the back EMF by nearly 8.5%.

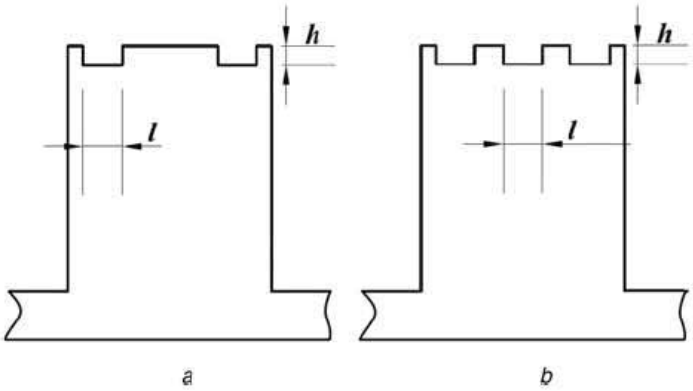

Figure 5 *Schematic of rotor tooth-notching*

a Two notches
b Three notches

3.2 Rotor tooth-chamfering

Rotor tooth-chamfering is commonly adopted in reluctance machines to reduce the armature reaction effect and improve the torque performance [27]. It can also be used to smoothen the variation of air-gap permeance $G(\alpha,z)$ in the PMFS machine, and resultantly suppress the cogging torque. Various chamfering radii (see Fig. 8), $R = 3$, 5 and 6 mm, denoted as 'cham1', 'cham2' and 'cham3', respectively, are studied for their effects in cogging torque reduction of the proposed PMFS ISG. The cogging torque and phase back EMF profiles of the machines are illustrated in Figs. 9 and 10, respectively. The results show that both the magnitude and phase angle of the cogging torque waveforms change along with the chamfering radius, and the reduction of back EMF becomes more severe as the chamfer radius decreases. It can be observed that the

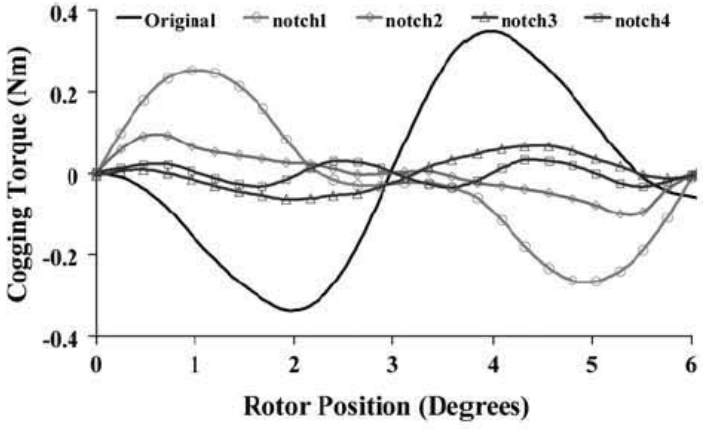

Figure 6 *Cogging torque profiles for rotor tooth-notching*

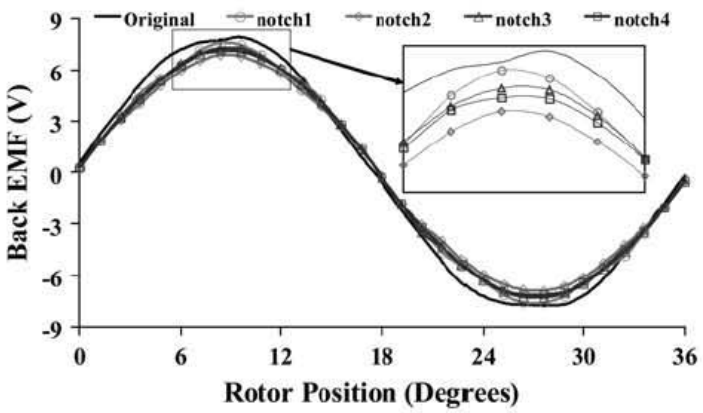

Figure 7 *Phase back EMF waveforms for rotor tooth-notching*

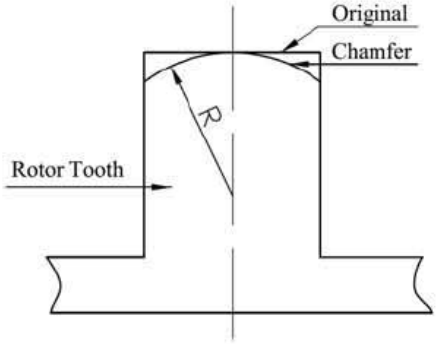

Figure 8 *Schematic of rotor tooth-chamfering*

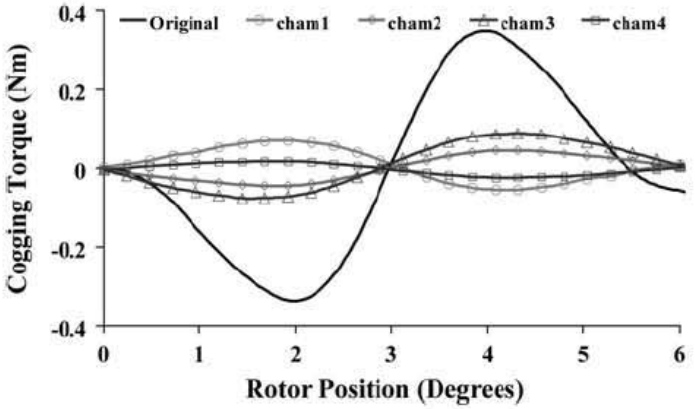

Figure 9 *Cogging torque profiles for rotor tooth-chamfering*

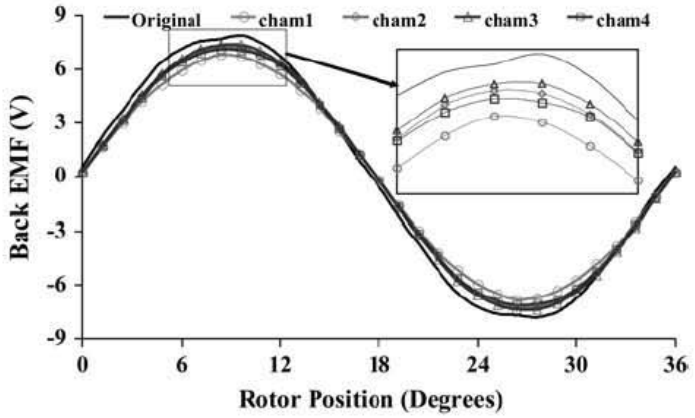

Figure 10 *Phase back EMF waveforms for rotor tooth-chamfering*

cogging torque profiles with 'cham1' and 'cham2' have almost the same magnitude but opposite polarities. Therefore an intermediate chamfering radius $R = 4.3$ mm, denoted as 'cham4', is obtainable through extensive FEA optimisation, and 'cham4' is found to be able to minimise the peak value of the cogging torque maximally to only 0.025 Nm, or about 7.5% of the original one, as shown in Fig. 9. However, it also decreases the peak value of the back EMF by 7.6% of the original as shown in Fig. 10.

3.3 Rotor tooth-pairing

Circumferential or axial magnets pairing have been implemented successfully in cogging torque reduction of PM brushless machines by some artful designs [22, 24, 28]. Since the cogging torque waveform varies with the rotor tooth width in PMFS machine [5, 7, 8], the rotor configuration with different tooth-widths assembled alternately as shown in Fig. 11, better known as rotor tooth-pairing, can be employed to alleviate the cogging torque effect in the proposed PMFS ISG. By using this technique, the air-gap permeance can be optimised in such a way that the integration of $G^2(\alpha, z)$ with α in (5) is minimised, resulting in a lower cogging torque. However, in such a design, the rotor mechanical balance should always be concerned.

The original rotor and two new rotors which will be used for tooth-paring are studied using FEA models. All teeth on each of the rotor are of the same width. The three rotor structures, with the ratio of the rotor tooth-width to the stator tooth-width being 1.6, 1.4 and 1.8, respectively, are denoted as 'original', 'ratio1.4' and 'ratio1.8' accordingly. The cogging torque profiles are shown in Fig. 12. It can be seen that the magnitude and phase angle of the cogging torque waveforms vary along with the rotor tooth-width. However, no polarity alteration is observed. Thus, it is predicted that the rotor tooth-pairing technique may reduce cogging torque less efficiently

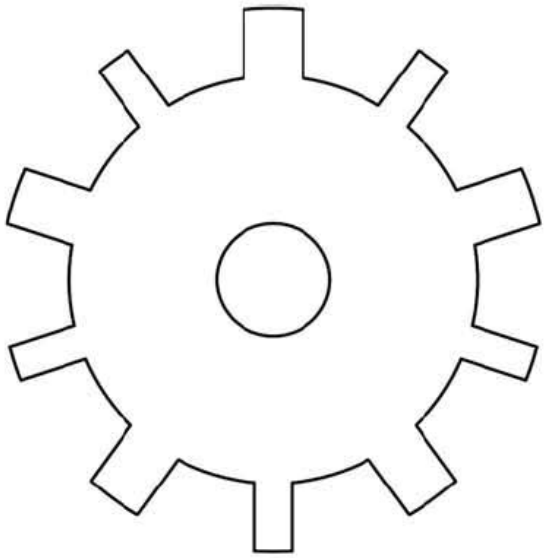

Figure 11 *Schematic of rotor tooth-pairing*

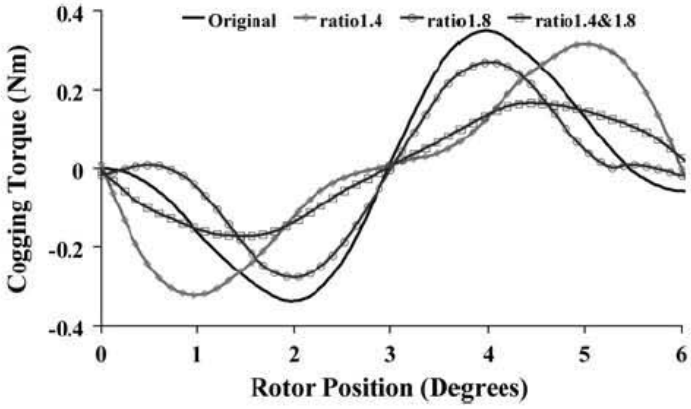

Figure 12 *Cogging torque profiles for rotor tooth-pairing*

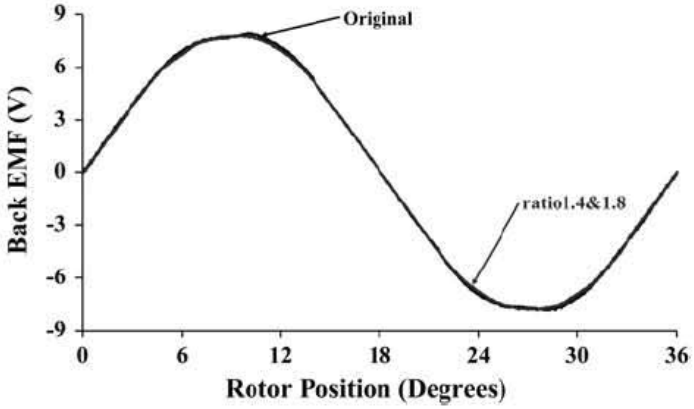

Figure 13 *Phase back EMF waveforms for rotor tooth-pairing*

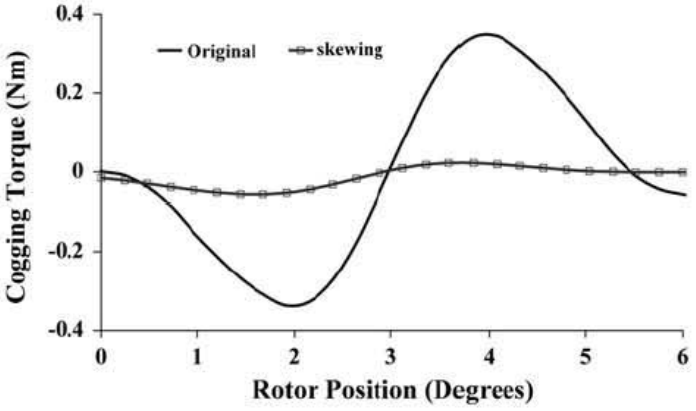

Figure 14 *Cogging torque profiles for rotor tooth-skewing*

compared with the previous methods. However, by way of example, an optimised rotor can be achieved by combining five teeth of 'ratio1.4' alternately with five teeth of 'ratio1.8', denoted as 'ratio1.4&1.8'. As can be seen from Fig. 12, it reduces the cogging torque peak value to 51% of the original. Moreover, it has negligible negative impact on the amplitude of the peak back EMF, as shown in Fig. 13.

However, it should be noted that for other machine topologies, it may be possible to find different rotor tooth-widths which lead to cogging torques with similar magnitude but opposite polarities, as in the previous methods. Thus, the rotor tooth-pairing technique will bring much better effect of cogging torque reduction.

3.4 Rotor tooth-skewing

Skewing of the stator or the rotor is the most common approach to reduce the cogging torque in PM machines [22–24]. For the PMFS under study, it is usually difficult to skew the stator since PM bars are embedded in it. However, it is practical to skew the rotor, which can optimise the air-gap permeance in such a way that the integration of $G^2(\alpha, z)$ with z in (5) is minimised, and the cogging torque is thus reduced. However, rotor tooth-skewing could decrease rotor saliency, which may lead to reduced back EMF and electromagnetic torque as well.

The original rotor is skewed by $\pi/30$, or one cogging torque period, for minimisation of cogging torque. Fig. 14 shows the FE-predicted waveforms of cogging torques before and after skewing, where the former waveform has been shown in Fig. 3. It is noted that the cogging torque is reduced by 89% using rotor tooth-skewing. In addition, it can be observed from Fig. 15 that the back EMF becomes more sinusoidal with less harmonic distortion, while the amplitude of back EMF drops only by 5.1%. These results show rotor tooth-skewing as an effective cogging torque reduction method for the PMFS.

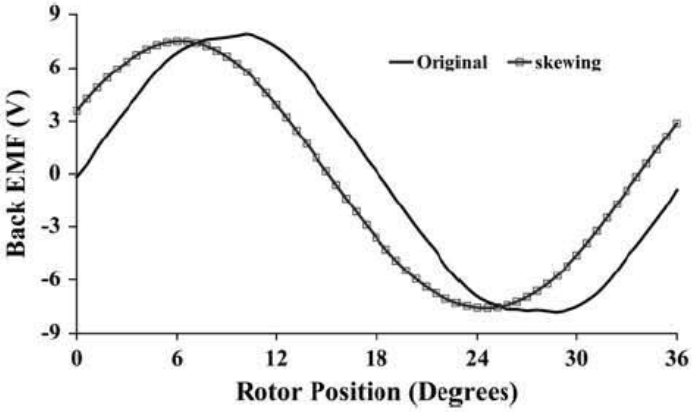

Figure 15 *Phase back EMF waveforms for rotor tooth-skewing*

4 Experimental validation

The prototypes of the five different rotor structures proposed in the preceding sections are shown in Fig. 16, which are used for experimental validations of the FEA models and the utility of the proposed cogging torque suppression methods in the PMFS ISG. The predicted cogging torque profiles from the FEA models and the experimental results for each of the four proposed techniques are individually compared in Fig. 17. Furthermore, peak-to-peak values of the cogging torque for different techniques are compared with the original one in Table 2. Ideally, all the proposed techniques assume prefect manufacture and assembly of the machine for their implementation. In practice, tight mechanical tolerances cannot always be met, and manufacturing and assembly deficiencies inevitably occur. In the prototype machines, it was found that some dimensions such as those of the PMs and lamination stacks which were manufactured by wire-cut, as well as the stator/rotor eccentricity, were not held to sufficient tolerances. These account for the noticeable deviations that occur between the FEA-predicted and measured results in Fig. 17. In the actual laboratory experiments, the rotor with tooth-chamfering was tested last. It was found that the measured cogging torque became higher every time the machine was disassembled and reassembled. This was attributed to the wear and tear of the bearing housings,

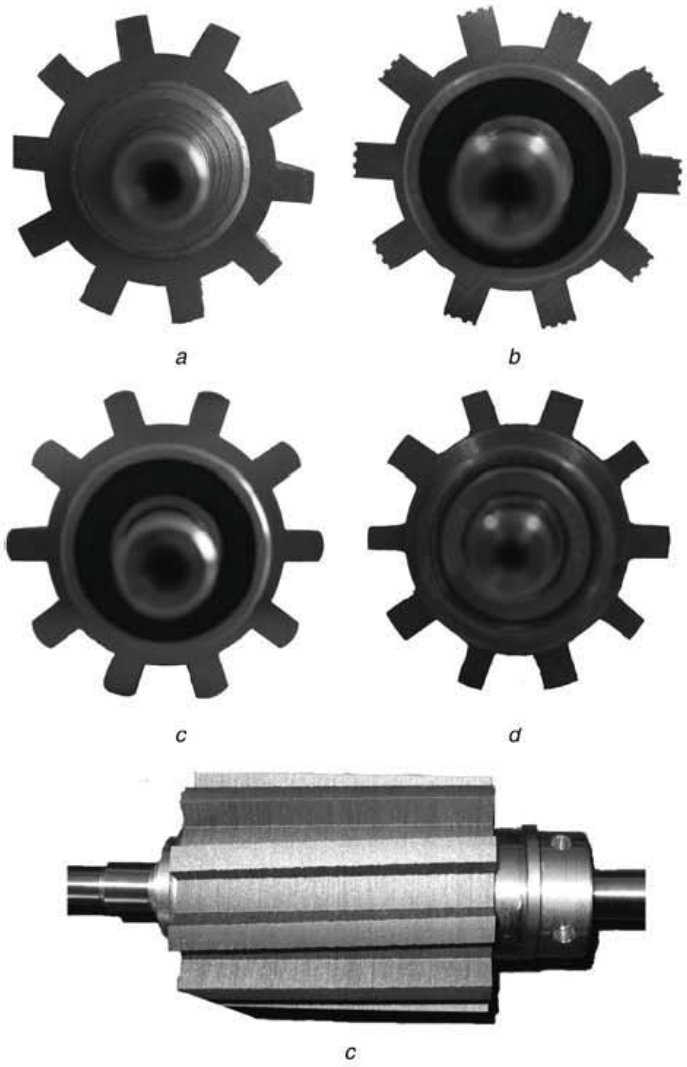

Figure 16 *Prototype rotors with different configurations*

a Original
b Tooth-notching
c Tooth-chamfering
d Tooth-pairing
e Tooth-skewing

which had been subjected to repeated assembly and disassembly from the previous tests. This also led to deteriorated eccentricity of the rotor and higher cogging torque. These effects are easily evident from the most noticeable deviation between the FEA and test results as shown in Fig. 17*b*. Moreover, only 2-D FE analysis was used to predict the cogging torque in the investigation, which means that the 3-D effects such as flux fringing in the machine have been neglected. This would also make the predicted results deviate from the test results. However, it can be seen that the all predicted cogging torque waveforms essentially show the same variations as the corresponding experimental results. The results in Table 2 show that the four design approaches can indeed reduce the cogging torque significantly by 89.0, 86.6, 59.5 and 87.2% from the original design, respectively. The effectiveness of the proposed measures for cogging torque reduction is thus fully demonstrated. The overall good agreements between the FEA and the experimental results have also confirmed the validity of the FEA models.

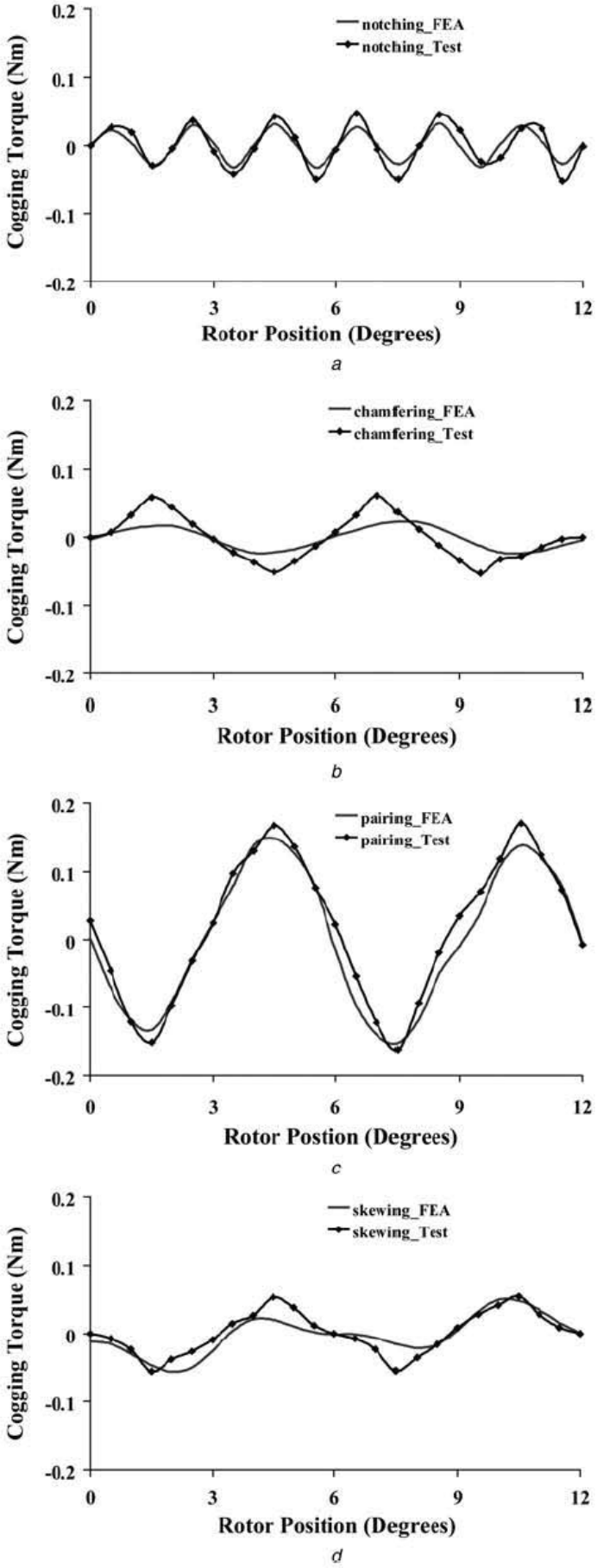

Figure 17 *Predicted and measured cogging torque profiles for various techniques*

a Tooth-notching
b Tooth-chamfering
c Tooth-pairing
d Tooth-skewing

Table 2 Cogging torque peak-to-peak value for the proposed techniques

Design techniques	FEA, Nm	Test, Nm	Percentage, % (test)
original	0.702	0.846	100
tooth-notching	0.061	0.093	11.0
tooth-chamfering	0.040	0.113	13.4
tooth-pairing	0.303	0.343	40.5
tooth-skewing	0.078	0.108	12.8

Additionally, the back EMFs of the machines with different rotors are measured at speed of 2400 rpm, as illustrated in Fig. 18. Since the experimental value of the back EMF are generally relatively less sensitive to mechanical defects and test bench measurements than in the case of low-level cogging torque, there are very close agreements between the experimental and predicted results. In order to investigate the back EMF further, harmonic analysis has been undertaken, and the fundamental values and total harmonics distortions (THD) are given in Table 3. The values of the fundamental component of the back EMF under the different techniques have found to be declined by 10.3, 9.2, 1.8 and 4.3, respectively. In addition, it can be seen that all the techniques, with the exception of rotor tooth-pairing, can ameliorate the THD of the back EMF, as shown in Table 3.

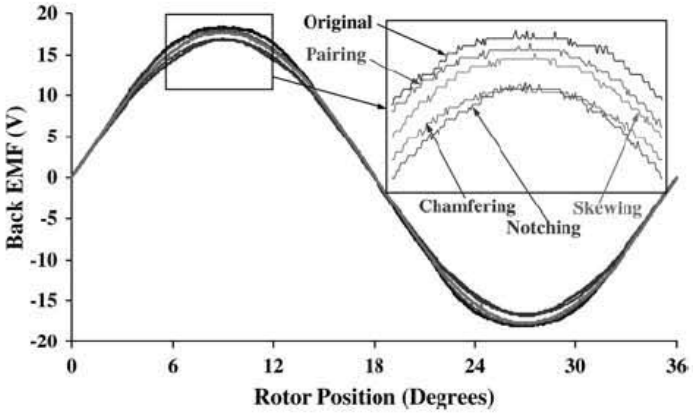

Figure 18 *Measured back-EMF waveforms for various design methods*

Table 3 Fundamental value and total harmonics distortion of measured back EMF

Design techniques	Fundamental, V	Percentage, %	THD, %
original	18.46	100	4.07
tooth-notching	16.55	89.7	2.46
tooth-chamfering	16.77	90.8	2.33
tooth-pairing	18.13	98.2	4.83
tooth-skewing	17.66	95.7	2.39

For better performance, it is generally more preferred to drive the machine in the brushless AC (BLAC) mode. A high THD value of back EMF would cause serious load-dependent torque ripple, which would compromise the effectiveness of cogging torque suppression. Therefore the technique for cogging torque reduction must also take into consideration other factors such as the THD of the back EMF. Tooth-skewing is considered as a favourite method for its effectiveness in cogging torque suppression with the least back EMF compromise, even though the assembly of the rotor is relatively complicated. From the foregoing comprehensive analysis and tests, it can be clearly seen that the proposed techniques can be applied for effective cogging torque reduction of the PMFS ISG under study, although at the expense of a small reduction of the back EMF. It is envisaged that the techniques can also be implemented cost effectively due to the simplicity of the rotor designs and assembly.

5 Conclusions

Four cogging torque suppression techniques, namely rotor tooth-notching, rotor tooth-chamfering, rotor tooth-pairing and rotor tooth-skewing, are investigated for a three-phase PMFS ISG with 12 stator poles and 10 rotor poles. Both the FEA and experimental results have revealed that the cogging torque can be effectively mitigated by all of the proposed techniques with minimum extra manufacture complexity and costs. The techniques will also lead to the undesirable effects of reduced back EMF, but they can also have a positive impact on the THD of back EMF. Thus, these factors should be taken into account for the implementation of the proposed techniques. Although the investigations have been undertaken on a PMFS ISG with specific configurations, it is envisaged that the proposed measures equally apply to other PMFS machines with different configurations. Further work should be undertaken to study the potential benefits of combining these measures together for more effective cogging torque reduction and better overall machine performance.

References

[1] WALKER A., ANPALAHAN P., COLES P., LAMPERTH M., RODGERT D.: 'Automotive integrated starter generator'. Proc. 2nd IEE Power Electronics, Machines and Drives Conf., March–April 2004, vol. 1, pp. 46–48

[2] CAI W.: 'Comparison and review of electric machines for integrated starter alternator applications'. Proc. 39th IEEE Industry Applications Conf., October 2004, vol. 1, pp. 386–393

[3] RAUCH S.E., JOHNSON L.J.: 'Design principles of flux-switching alternators', *AIEE Trans.*, 1955, **74**, (3), pp. 1261–1268

[4] HOANG E., BEN AHMED A.H., LUCIDARME J.: 'Switching flux permanent magnet polyphased synchronous machines'. Proc. 7th European Power Electronics and Applications Conf., 1997, pp. 903–908

[5] FANG Z.X., WANG Y., SHEN J.X., HUANG Z.W.: 'Design and analysis of a novel flux-switching permanent magnet integrated-starter-generator'. Proc. 4th IET Power Electronics, Machines and Drives Conf., April 2008, pp. 106–110

[6] AMARA Y., HOANG E., GABSI M., LECRIVAIN M., ALLANO S.: 'Design and comparison of different flux-switch synchronous machines for an aircraft oil breather application', *Euro. Trans. Electr. Power*, 2005, **15**, (6), pp. 497–511

[7] FEI W., SHEN J.X.: 'Novel permanent magnet switching flux motors'. Proc. 41st UPEC Conf., September 2006, vol. 2, pp. 729–733

[8] FEI W., SHEN J.X.: 'Comparative study and optimal design of PM switching flux motors'. Proc. 41st UPEC Conf., September 2006, vol. 2, pp. 695–699

[9] HUA W., ZHU Z.Q., CHENG M., PANG Y., HOWE D.: 'Comparison of flux-switching and doubly-salient permanent magnet brushless machines'. Proc. 8th Int. Electrical Machines and Systems Conf., September 2005, vol. 1, pp. 165–170

[10] HUA W., CHENG M., ZHU Z.Q., HOWE D.: 'Design of flux-switching permanent magnet machine considering the limitation of inverter and flux-weakening capability'. Proc. 41st IEEE Industry Application Society Annual Conf., October 2006, vol. 5, pp. 2403–2410

[11] HUA W., CHENG M.: 'Inductance characteristics of 3-phase flux-switching permanent magnet machine with doubly-salient structure'. Proc. 5th IEEE Int. Power Electronics and Motion Control Conf., August 2006, vol. 3, pp. 1–5

[12] HUA W., CHENG M., ZHU Z.Q., HOWE D.: 'Analysis and optimization of back-EMF waveform of a novel flux-switching permanent magnet motor'. Proc. IEEE Int. Electric Machines and Drives Conf., May 2007, vol. 2, pp. 1025–1030

[13] ZHU Z.Q., PANG Y., HOWE D., IWASAKI S., DEODHAR R., PRIDE A.: 'Analysis of electromagnetic performance of flux-switching permanent-magnet machines by nonlinear adaptive lumped parameter magnetic circuit model', *IEEE Trans. Magn.*, 2005, **41**, (11), pp. 4277–4287

[14] ZHU Z.Q., PANG Y., CHEN J.T., *ET AL.*: 'Analysis and reduction of magnet eddy current loss in flux-switching permanent magnet machines'. Proc. 4th IET Power Electronics, Machines and Drives Conf., April 2008, pp. 120–124

[15] ZHU Z.Q., PANG Y., CHEN J.T., XIA Z.P., HOWE D.: 'Influence of design parameters on output torque of flux-switching permanent magnet machines'. Proc. IEEE Vehicle Power and Propulsion Conf., September 2008, pp. 1–6

[16] THOMAS A., ZHU Z.Q., JEWELL G.W., HOWE D.: 'Flux-switching PM brushless machines with alternative stator and rotor pole combinations'. Proc. 11th Int. Electrical Machines and Systems Conf., October 2008, pp. 2986–2991

[17] OCHIJE K.N., POLLOCK C.: 'Design/performance of a flux switching generator system for variable speed applications'. Proc. 40th IEEE Industry Application Annual Conf., October 2005, vol. 3, pp. 1567–1574

[18] CHEN Y., ZHU Z.Q., HOWE D.: 'Three-dimensional lumped-parameter magnetic circuit analysis of single-phase flux-switching permanent-magnet motor', *IEEE Trans. Ind. Appl.*, 2008, **44**, (6), pp. 1701–1710

[19] CHAI K.S., POLLOCK C.: 'Using genetic algorithms in design optimization of the flux switching motor'. Proc. IEEE Int. Power Electronics, Machines and Drives Conf., June 2002, pp. 540–545

[20] HUA W., CHENG M.: 'Cogging torque reduction of flux-switching permanent magnet machines without skewing'. Proc. 11th Int. Electrical Machines and Systems Conf., October 2008, pp. 3020–3025

[21] WANG C.F., SHEN J.X., WANG Y., WANG L.L., JIN M.J.: 'A new method for reduction of detent force in permanent magnet flux-switching linear motors', *IEEE Trans. Magn.*, 2009, **45**, (6), pp. 2843–2846

[22] BIANCHI N., BOLOGNANI S.: 'Design techniques for reducing the cogging torque in surface-mounted PM motors', *IEEE Trans. Ind. Appl.*, 2002, **38**, (5), pp. 1259–1265

[23] DOSIEK L., PILLAY P.: 'Cogging torque reduction in permanent magnet machines', *IEEE Trans. Ind. Appl.*, 2007, **43**, (6), pp. 1565–1571

[24] FEI W., LUK P.C.K.: 'A new technique of cogging torque suppression in direct-drive permanent magnet brushless machines'. Proc. IEEE Int. Electric Machines and Drives Conf., May 2009, pp. 9–16

[25] ZHU L., JIANG S.Z., ZHU Z.Q., CHAN C.C.: 'Analytical methods for minimizing cogging torque in permanent-magnet machines', *IEEE Trans. Magn.*, 2009, **45**, (4), pp. 2023–2031

[26] KANG G., SON Y., KIM G., HUR J.: 'A novel cogging torque reduction method for interior-type permanent-magnet motor', *IEEE Trans. Ind. Appl.*, 2009, **45**, (1), pp. 161–167

[27] RAKGATI E.T., KAMPER M.J., LE ROUX A.D.: 'Torque performance of optimally designed six-phase reluctance DC machine'. Proc. 41st IEEE Industry Application Society Annual Conf., October 2006, vol. 3, pp. 1186–1192

[28] KIM T.H., WON S.H., JU K.B., LEE J.: 'Reduction of cogging torque in flux-reversal machine by rotor teeth pairing', *IEEE Trans. Magn.*, 2005, **41**, (10), pp. 3964–3966

Cogging torque suppression in a permanent-magnet flux-switching integrated-starte

Jin, Meng-Jia

2010-09-13T00:00:00Z

Jin M-J, Wang Y, Shen X-J, et al., (2010) Cogging torque suppression in a permanent-magnet flux-switching integrated-starter-generator. IET Electric Power Applications, Volume 4, Issue 8, 2010, pp. 647-656

http://dx.doi.org/10.1049/iet-epa.2009.0176